

Search for large extra spatial dimensions in the dielectron and diphoton channels in $p\bar{p}$ collisions at $\sqrt{s} = 1.96$ TeV

V.M. Abazov³⁶, B. Abbott⁷⁵, M. Abolins⁶⁵, B.S. Acharya²⁹, M. Adams⁵¹, T. Adams⁴⁹, E. Aguilo⁶, M. Ahsan⁵⁹, G.D. Alexeev³⁶, G. Alkhazov⁴⁰, A. Alton^{64,a}, G. Alverson⁶³, G.A. Alves², M. Anastasoaie³⁵, L.S. Ancu³⁵, T. Andeen⁵³, B. Andrieu¹⁷, M.S. Anzelc⁵³, M. Aoki⁵⁰, Y. Arnoud¹⁴, M. Arov⁶⁰, M. Arthaud¹⁸, A. Askew⁴⁹, B. Åsman⁴¹, A.C.S. Assis Jesus³, O. Atramentov⁴⁹, C. Avila⁸, F. Badaud¹³, L. Bagby⁵⁰, B. Baldin⁵⁰, D.V. Bandurin⁵⁹, P. Banerjee²⁹, S. Banerjee²⁹, E. Barberis⁶³, A.-F. Barfuss¹⁵, P. Bargassa⁸⁰, P. Baringer⁵⁸, J. Barreto², J.F. Bartlett⁵⁰, U. Bassler¹⁸, D. Bauer⁴³, S. Beale⁶, A. Bean⁵⁸, M. Begalli³, M. Begel⁷³, C. Belanger-Champagne⁴¹, L. Bellantoni⁵⁰, A. Bellavance⁵⁰, J.A. Benitez⁶⁵, S.B. Beri²⁷, G. Bernardi¹⁷, R. Bernhard²³, I. Bertram⁴², M. Besançon¹⁸, R. Beuselinck⁴³, V.A. Bezzubov³⁹, P.C. Bhat⁵⁰, V. Bhatnagar²⁷, C. Biscarat²⁰, G. Blazey⁵², F. Blekman⁴³, S. Blessing⁴⁹, K. Bloom⁶⁷, A. Boehlein⁵⁰, D. Boline⁶², T.A. Bolton⁵⁹, E.E. Boos³⁸, G. Borissov⁴², T. Bose⁷⁷, A. Brandt⁷⁸, R. Brock⁶⁵, G. Brooijmans⁷⁰, A. Bross⁵⁰, D. Brown⁸¹, X.B. Bu⁷, N.J. Buchanan⁴⁹, D. Buchholz⁵³, M. Buehler⁸¹, V. Buescher²², V. Bunichev³⁸, S. Burdin^{42,b}, T.H. Burnett⁸², C.P. Buszello⁴³, J.M. Butler⁶², P. Calfayan²⁵, S. Calvet¹⁶, J. Cammin⁷¹, M.A. Carrasco-Lizarraga³³, E. Carrera⁴⁹, W. Carvalho³, B.C.K. Casey⁵⁰, H. Castilla-Valdez³³, S. Chakrabarti¹⁸, D. Chakraborty⁵², K.M. Chan⁵⁵, A. Chandra⁴⁸, E. Cheu⁴⁵, F. Chevallier¹⁴, D.K. Cho⁶², S. Choi³², B. Choudhary²⁸, L. Christofek⁷⁷, T. Christoudias⁴³, S. Cihangir⁵⁰, D. Claes⁶⁷, J. Clutter⁵⁸, M. Cooke⁵⁰, W.E. Cooper⁵⁰, M. Corcoran⁸⁰, F. Couderc¹⁸, M.-C. Cousinou¹⁵, S. Crépé-Renaudin¹⁴, V. Cuplov⁵⁹, D. Cutts⁷⁷, M. Ćwiok³⁰, H. da Motta², A. Das⁴⁵, G. Davies⁴³, K. De⁷⁸, S.J. de Jong³⁵, E. De La Cruz-Burelo³³, C. De Oliveira Martins³, K. DeVaughan⁶⁷, F. Déliot¹⁸, M. Demarteau⁵⁰, R. Demina⁷¹, D. Denisov⁵⁰, S.P. Denisov³⁹, S. Desai⁵⁰, H.T. Diehl⁵⁰, M. Diesburg⁵⁰, A. Dominguez⁶⁷, T. Dorland⁸², A. Dubey²⁸, L.V. Dudko³⁸, L. Duflot¹⁶, S.R. Dugad²⁹, D. Duggan⁴⁹, A. Duperrin¹⁵, J. Dyer⁶⁵, A. Dyshkant⁵², M. Eads⁶⁷, D. Edmunds⁶⁵, J. Ellison⁴⁸, V.D. Elvira⁵⁰, Y. Enari⁷⁷, S. Eno⁶¹, P. Ermolov^{38,‡}, H. Evans⁵⁴, A. Evdokimov⁷³, V.N. Evdokimov³⁹, A.V. Ferapontov⁵⁹, T. Ferbel⁷¹, F. Fiedler²⁴, F. Filthaut³⁵, W. Fisher⁵⁰, H.E. Fisk⁵⁰, M. Fortner⁵², H. Fox⁴², S. Fu⁵⁰, S. Fuess⁵⁰, T. Gadfort⁷⁰, C.F. Galea³⁵, C. Garcia⁷¹, A. Garcia-Bellido⁷¹, V. Gavrilov³⁷, P. Gay¹³, W. Geist¹⁹, W. Geng^{15,65}, C.E. Gerber⁵¹, Y. Gershtein^{49,c}, D. Gillberg⁶, G. Ginther⁷¹, B. Gómez⁸, A. Goussiou⁸², P.D. Grannis⁷², H. Greenlee⁵⁰, Z.D. Greenwood⁶⁰, E.M. Gregores⁴, G. Grenier²⁰, Ph. Gris¹³, J.-F. Grivaz¹⁶, A. Grohsjean²⁵, S. Grünendahl⁵⁰, M.W. Grünewald³⁰, F. Guo⁷², J. Guo⁷², G. Gutierrez⁵⁰, P. Gutierrez⁷⁵, A. Haas⁷⁰, N.J. Hadley⁶¹, P. Haefner²⁵, S. Hagopian⁴⁹, J. Haley⁶⁸, I. Hall⁶⁵, R.E. Hall⁴⁷, L. Han⁷, K. Harder⁴⁴, A. Harel⁷¹, J.M. Hauptman⁵⁷, J. Hays⁴³, T. Hebbeker²¹, D. Hedin⁵², J.G. Hegeman³⁴, A.P. Heinson⁴⁸, U. Heintz⁶², C. Hensel^{22,d}, K. Herner⁷², G. Hesketh⁶³, M.D. Hildreth⁵⁵, R. Hirosky⁸¹, J.D. Hobbs⁷², B. Hoeneisen¹², M. Hohlfeld²², S. Hossain⁷⁵, P. Houben³⁴, Y. Hu⁷², Z. Hubacek¹⁰, V. Hynek⁹, I. Iashvili⁶⁹, R. Illingworth⁵⁰, A.S. Ito⁵⁰, S. Jabeen⁶², M. Jaffré¹⁶, S. Jain⁷⁵, K. Jakobs²³, C. Jarvis⁶¹, R. Jesik⁴³, K. Johns⁴⁵, C. Johnson⁷⁰, M. Johnson⁵⁰, D. Johnston⁶⁷, A. Jonckheere⁵⁰, P. Jonsson⁴³, A. Juste⁵⁰, E. Kajfasz¹⁵, D. Karmanov³⁸, P.A. Kasper⁵⁰, I. Katsanos⁷⁰, D. Kau⁴⁹, V. Kaushik⁷⁸, R. Kehoe⁷⁹, S. Kermiche¹⁵, N. Khalatyan⁵⁰, A. Khanov⁷⁶, A. Kharchilava⁶⁹, Y.M. Kharzeev³⁶, D. Khatidze⁷⁰, T.J. Kim³¹, M.H. Kirby⁵³, M. Kirsch²¹, B. Klíma⁵⁰, J.M. Kohli²⁷, J.-P. Konrath²³, A.V. Kozelov³⁹, J. Kraus⁶⁵, T. Kuhl²⁴, A. Kumar⁶⁹, A. Kupco¹¹, T. Kurča²⁰, V.A. Kuzmin³⁸, J. Kvita⁹, F. Lacroix¹³, D. Lam⁵⁵, S. Lammers⁷⁰, G. Landsberg⁷⁷, P. Lebrun²⁰, W.M. Lee⁵⁰, A. Leflat³⁸, J. Lellouch¹⁷, J. Li^{78,‡}, L. Li⁴⁸, Q.Z. Li⁵⁰, S.M. Lietti⁵, J.K. Lim³¹, J.G.R. Lima⁵², D. Lincoln⁵⁰, J. Linnemann⁶⁵, V.V. Lipaev³⁹, R. Lipton⁵⁰, Y. Liu⁷, Z. Liu⁶, A. Lobodenko⁴⁰, M. Lokajicek¹¹, P. Love⁴², H.J. Lubatti⁸², R. Luna-Garcia^{33, e}, A.L. Lyon⁵⁰, A.K.A. Maciel², D. Mackin⁸⁰, R.J. Madaras⁴⁶, P. Mättig²⁶, C. Magass²¹, A. Magerkurth⁶⁴, P.K. Mal⁸², H.B. Malbouisson³, S. Malik⁶⁷, V.L. Malyshev³⁶, Y. Maravin⁵⁹, B. Martin¹⁴, R. McCarthy⁷², M.M. Meijer³⁵, A. Melnitchouk⁶⁶, L. Mendoza⁸, P.G. Mercadante⁵, M. Merkin³⁸, K.W. Merritt⁵⁰, A. Meyer²¹, J. Meyer^{22,d}, J. Mitrevski⁷⁰, R.K. Mommsen⁴⁴, N.K. Mondal²⁹, R.W. Moore⁶, T. Moulik⁵⁸, G.S. Muanza¹⁵, M. Mulhearn⁷⁰, O. Mundal²², L. Mundim³, E. Nagy¹⁵, M. Naimuddin⁵⁰, M. Narain⁷⁷, N.A. Naumann³⁵, H.A. Neal⁶⁴, J.P. Negret⁸, P. Neustroev⁴⁰, H. Nilsen²³, H. Nogima³, S.F. Novaes⁵, T. Nunnemann²⁵, V. O'Dell⁵⁰, D.C. O'Neil⁶, G. Obrant⁴⁰, C. Ochando¹⁶, D. Onoprienko⁵⁹, N. Oshima⁵⁰, N. Osman⁴³, J. Osta⁵⁵, R. Otec¹⁰, G.J. Otero y Garzón⁵⁰, M. Owen⁴⁴, P. Padley⁸⁰, M. Pangilinan⁷⁷, N. Parashar⁵⁶, S.-J. Park^{22,d}, S.K. Park³¹, J. Parsons⁷⁰, R. Partridge⁷⁷, N. Parua⁵⁴, A. Patwa⁷³, G. Pawloski⁸⁰, B. Penning²³, M. Perfilov³⁸, K. Peters⁴⁴, Y. Peters²⁶, P. Pétreoff¹⁶, M. Petteni⁴³, R. Piegaia¹, J. Piper⁶⁵, M.-A. Pleier²², P.L.M. Podesta-Lerma^{33,f}, V.M. Podstavkov⁵⁰, Y. Pogorelov⁵⁵, M.-E. Pol², P. Polozov³⁷, B.G. Pope⁶⁵, A.V. Popov³⁹, C. Potter⁶, W.L. Prado da Silva³, H.B. Prosper⁴⁹, S. Protopopescu⁷³, J. Qian⁶⁴, A. Quadt^{22,d}, B. Quinn⁶⁶, A. Rakitine⁴², M.S. Rangel², K. Ranjan²⁸, P.N. Ratoff⁴², P. Renkel⁷⁹, P. Rich⁴⁴, M. Rijssenbeek⁷², I. Ripp-Baudot¹⁹, F. Rizatdinova⁷⁶, S. Robinson⁴³, R.F. Rodrigues³, M. Rominsky⁷⁵, C. Royon¹⁸, P. Rubinov⁵⁰, R. Ruchti⁵⁵,

G. Safronov³⁷, G. Sajot¹⁴, A. Sánchez-Hernández³³, M.P. Sanders¹⁷, B. Sanghi⁵⁰, G. Savage⁵⁰, L. Sawyer⁶⁰, T. Scanlon⁴³, D. Schaile²⁵, R.D. Schamberger⁷², Y. Scheglov⁴⁰, H. Schellman⁵³, T. Schliephake²⁶, S. Schlobohm⁸², C. Schwanenberger⁴⁴, A. Schwartzman⁶⁸, R. Schwienhorst⁶⁵, J. Sekarić⁴⁹, H. Severini⁷⁵, E. Shabalina⁵¹, M. Shamim⁵⁹, V. Shary¹⁸, A.A. Shchukin³⁹, R.K. Shivpuri²⁸, V. Siccardi¹⁹, V. Simak¹⁰, V. Sirotenko⁵⁰, P. Skubic⁷⁵, P. Slattery⁷¹, D. Smirnov⁵⁵, G.R. Snow⁶⁷, J. Snow⁷⁴, S. Snyder⁷³, S. Söldner-Rembold⁴⁴, L. Sonnenschein¹⁷, A. Sopczak⁴², M. Sosebee⁷⁸, K. Soustruznik⁹, B. Spurlock⁷⁸, J. Stark¹⁴, V. Stolin³⁷, D.A. Stoyanova³⁹, J. Strandberg⁶⁴, S. Strandberg⁴¹, M.A. Strang⁶⁹, E. Strauss⁷², M. Strauss⁷⁵, R. Ströhmer²⁵, D. Strom⁵³, L. Stutte⁵⁰, S. Sumowidagdo⁴⁹, P. Svoisky³⁵, A. Sznajder³, A. Tanasijczuk¹, W. Taylor⁶, B. Tiller²⁵, F. Tissandier¹³, M. Titov¹⁸, V.V. Tokmenin³⁶, I. Torchiani²³, D. Tsybychev⁷², B. Tuchming¹⁸, C. Tully⁶⁸, P.M. Tuts⁷⁰, R. Unalan⁶⁵, L. Uvarov⁴⁰, S. Uvarov⁴⁰, S. Uzunyan⁵², B. Vachon⁶, P.J. van den Berg³⁴, R. Van Kooten⁵⁴, W.M. van Leeuwen³⁴, N. Varelas⁵¹, E.W. Varnes⁴⁵, I.A. Vasilyev³⁹, P. Verdier²⁰, L.S. Vertogradov³⁶, M. Verzocchi⁵⁰, D. Vilanova¹⁸, F. Villeneuve-Seguier⁴³, P. Vint⁴³, P. Vokac¹⁰, M. Voutilainen^{67,g}, R. Wagner⁶⁸, H.D. Wahl⁴⁹, M.H.L.S. Wang⁵⁰, J. Warchol⁵⁵, G. Watts⁸², M. Wayne⁵⁵, G. Weber²⁴, M. Weber^{50,h}, L. Welty-Rieger⁵⁴, A. Wenger^{23,i}, N. Wermes²², M. Wetstein⁶¹, A. White⁷⁸, D. Wicke²⁶, M. Williams⁴², G.W. Wilson⁵⁸, S.J. Wimpenny⁴⁸, M. Wobisch⁶⁰, D.R. Wood⁶³, T.R. Wyatt⁴⁴, Y. Xie⁷⁷, C. Xu⁶⁴, S. Yacoob⁵³, R. Yamada⁵⁰, W.-C. Yang⁴⁴, T. Yasuda⁵⁰, Y.A. Yatsunenko³⁶, H. Yin⁷, K. Yip⁷³, H.D. Yoo⁷⁷, S.W. Youn⁵³, J. Yu⁷⁸, C. Zeitnitz²⁶, S. Zelitch⁸¹, T. Zhao⁸², B. Zhou⁶⁴, J. Zhu⁷², M. Zielinski⁷¹, D. Ziemińska⁵⁴, A. Ziemiński^{54,†}, L. Zivkovic⁷⁰, V. Zutshi⁵², and E.G. Zverev³⁸

(The *DØ* Collaboration)

¹Universidad de Buenos Aires, Buenos Aires, Argentina

²LAFEX, Centro Brasileiro de Pesquisas Físicas, Rio de Janeiro, Brazil

³Universidade do Estado do Rio de Janeiro, Rio de Janeiro, Brazil

⁴Universidade Federal do ABC, Santo André, Brazil

⁵Instituto de Física Teórica, Universidade Estadual Paulista, São Paulo, Brazil

⁶University of Alberta, Edmonton, Alberta, Canada, Simon Fraser University,

Burnaby, British Columbia, Canada, York University, Toronto,

Ontario, Canada, and McGill University, Montreal, Quebec, Canada

⁷University of Science and Technology of China, Hefei, People's Republic of China

⁸Universidad de los Andes, Bogotá, Colombia

⁹Center for Particle Physics, Charles University, Prague, Czech Republic

¹⁰Czech Technical University, Prague, Czech Republic

¹¹Center for Particle Physics, Institute of Physics, Academy of Sciences of the Czech Republic, Prague, Czech Republic

¹²Universidad San Francisco de Quito, Quito, Ecuador

¹³LPC, Université Blaise Pascal, CNRS/IN2P3, Clermont, France

¹⁴LPSC, Université Joseph Fourier Grenoble 1, CNRS/IN2P3,

Institut National Polytechnique de Grenoble, Grenoble, France

¹⁵CPPM, Aix-Marseille Université, CNRS/IN2P3, Marseille, France

¹⁶LAL, Université Paris-Sud, IN2P3/CNRS, Orsay, France

¹⁷LPNHE, IN2P3/CNRS, Universités Paris VI and VII, Paris, France

¹⁸CEA, Irfu, SPP, Saclay, France

¹⁹IPHC, Université Louis Pasteur, CNRS/IN2P3, Strasbourg, France

²⁰IPNL, Université Lyon 1, CNRS/IN2P3, Villeurbanne, France and Université de Lyon, Lyon, France

²¹III. Physikalisches Institut A, RWTH Aachen University, Aachen, Germany

²²Physikalisches Institut, Universität Bonn, Bonn, Germany

²³Physikalisches Institut, Universität Freiburg, Freiburg, Germany

²⁴Institut für Physik, Universität Mainz, Mainz, Germany

²⁵Ludwig-Maximilians-Universität München, München, Germany

²⁶Fachbereich Physik, University of Wuppertal, Wuppertal, Germany

²⁷Panjab University, Chandigarh, India

²⁸Delhi University, Delhi, India

²⁹Tata Institute of Fundamental Research, Mumbai, India

³⁰University College Dublin, Dublin, Ireland

³¹Korea Detector Laboratory, Korea University, Seoul, Korea

³²SungKyunKwan University, Suwon, Korea

³³CINVESTAV, Mexico City, Mexico

³⁴FOM-Institute NIKHEF and University of Amsterdam/NIKHEF, Amsterdam, The Netherlands

³⁵Radboud University Nijmegen/NIKHEF, Nijmegen, The Netherlands

³⁶Joint Institute for Nuclear Research, Dubna, Russia

³⁷Institute for Theoretical and Experimental Physics, Moscow, Russia

³⁸Moscow State University, Moscow, Russia

³⁹Institute for High Energy Physics, Protvino, Russia

- ⁴⁰Petersburg Nuclear Physics Institute, St. Petersburg, Russia
⁴¹Lund University, Lund, Sweden, Royal Institute of Technology and Stockholm University, Stockholm, Sweden, and Uppsala University, Uppsala, Sweden
⁴²Lancaster University, Lancaster, United Kingdom
⁴³Imperial College, London, United Kingdom
⁴⁴University of Manchester, Manchester, United Kingdom
⁴⁵University of Arizona, Tucson, Arizona 85721, USA
⁴⁶Lawrence Berkeley National Laboratory and University of California, Berkeley, California 94720, USA
⁴⁷California State University, Fresno, California 93740, USA
⁴⁸University of California, Riverside, California 92521, USA
⁴⁹Florida State University, Tallahassee, Florida 32306, USA
⁵⁰Fermi National Accelerator Laboratory, Batavia, Illinois 60510, USA
⁵¹University of Illinois at Chicago, Chicago, Illinois 60607, USA
⁵²Northern Illinois University, DeKalb, Illinois 60115, USA
⁵³Northwestern University, Evanston, Illinois 60208, USA
⁵⁴Indiana University, Bloomington, Indiana 47405, USA
⁵⁵University of Notre Dame, Notre Dame, Indiana 46556, USA
⁵⁶Purdue University Calumet, Hammond, Indiana 46323, USA
⁵⁷Iowa State University, Ames, Iowa 50011, USA
⁵⁸University of Kansas, Lawrence, Kansas 66045, USA
⁵⁹Kansas State University, Manhattan, Kansas 66506, USA
⁶⁰Louisiana Tech University, Ruston, Louisiana 71272, USA
⁶¹University of Maryland, College Park, Maryland 20742, USA
⁶²Boston University, Boston, Massachusetts 02215, USA
⁶³Northeastern University, Boston, Massachusetts 02115, USA
⁶⁴University of Michigan, Ann Arbor, Michigan 48109, USA
⁶⁵Michigan State University, East Lansing, Michigan 48824, USA
⁶⁶University of Mississippi, University, Mississippi 38677, USA
⁶⁷University of Nebraska, Lincoln, Nebraska 68588, USA
⁶⁸Princeton University, Princeton, New Jersey 08544, USA
⁶⁹State University of New York, Buffalo, New York 14260, USA
⁷⁰Columbia University, New York, New York 10027, USA
⁷¹University of Rochester, Rochester, New York 14627, USA
⁷²State University of New York, Stony Brook, New York 11794, USA
⁷³Brookhaven National Laboratory, Upton, New York 11973, USA
⁷⁴Langston University, Langston, Oklahoma 73050, USA
⁷⁵University of Oklahoma, Norman, Oklahoma 73019, USA
⁷⁶Oklahoma State University, Stillwater, Oklahoma 74078, USA
⁷⁷Brown University, Providence, Rhode Island 02912, USA
⁷⁸University of Texas, Arlington, Texas 76019, USA
⁷⁹Southern Methodist University, Dallas, Texas 75275, USA
⁸⁰Rice University, Houston, Texas 77005, USA
⁸¹University of Virginia, Charlottesville, Virginia 22901, USA and
⁸²University of Washington, Seattle, Washington 98195, USA

(Dated: Sep 16, 2008)

We report on a search for large extra spatial dimensions in the dielectron and diphoton channels using a data sample of 1.05 fb^{-1} of $p\bar{p}$ collisions at a center-of-mass energy of 1.96 TeV collected by the D0 detector at the Fermilab Tevatron Collider. The invariant mass spectrum of the data agrees well with the prediction of the standard model. We find 95% C.L. lower limits on the effective Planck scale between 2.1 and 1.3 TeV for 2 to 7 extra dimensions.

PACS numbers: 04.50+h, 04.80.Cc, 11.25.Mj, 13.85.Rm, 11.10.Kk, 13.40.Hq

Within the standard model (SM) the mass of Higgs boson is unstable against radiative corrections. The fact that the mass is not of the order of the GUT or Planck scales at 10^{16} or 10^{19} GeV but rather $\mathcal{O}(10^2 \text{ GeV})$ is commonly referred to as the “hierarchy problem”. One way to circumvent the need for such fine tuning in the Higgs mass is by extending the dimensionality of the space, as in the large extra dimension model (LED) proposed by Arkani-Hamed, Dimopoulos and Dvali

(ADD) [1], which posits that the fields of the standard model are pinned to a $(3 + 1)$ -dimensional membrane, while gravity propagates in n_d additional compactified spatial dimensions. Gauss’ Law gives the relation between the fundamental Planck scale M_D , the observed Planck scale M_{Pl} , and the size of the extra dimensions R : $[M_{\text{Pl}}]^2 \approx R^{n_d} [M_D]^{n_d+2}$. If R is large compared to the Planck length $\simeq 1.6 \times 10^{-33} \text{ cm}$, M_D can be as low as $\mathcal{O}(1 \text{ TeV})$, thus avoiding the hierarchy prob-

lem and making gravity strong at the TeV scale. Extra spatial dimensions will manifest themselves by the presence of a series of graviton states, known as a “Kaluza-Klein tower”, (G_{KK}). At colliders, large extra dimensions can be probed by searching for the effect of G_{KK} on fermion or boson pair production [2].

Extra dimension amplitudes will result in enhancement of the cross sections above the SM values, especially at high energies. The LED cross section, which consists of SM, interference, and direct gravity terms, can be parametrized by a single variable $\eta_G = F/M_s^4$ where M_s is the the effective Planck scale, the ultraviolet cutoff of the sum over Kaluza-Klein states in virtual graviton exchange. The exact relationship between M_s and M_D depends on the exact quantum gravity scenario although they are of the same order of magnitude. The dimensionless parameter F to leading order (LO) and the sub-leading n_d dependence is given by

$$F = 1, \text{ (GRW [3])} \quad (1)$$

$$F = \begin{cases} \ln(M_s^2/\hat{s}) \text{ for } n_d = 2, \\ \frac{2}{n_d - 2} \text{ for } n_d > 2 \end{cases} \text{ (HLZ [4])} \quad (2)$$

where \hat{s} is the center of mass energy of the partonic subprocess.

In this Letter, we present a search for LED performed in events containing an e^+e^- or $\gamma\gamma$ pair with 1.05 fb^{-1} of $p\bar{p}$ collider data collected with the upgraded D0 detector [5] between October 2002 and February 2006. With 127 pb^{-1} of data, D0 has published limits on M_s ranging from 0.97 to 1.44 TeV for $n_d = 7 - 2$ in the combined dielectron and diphoton channels [6]. D0 has also published limits in the dimuon channel with 246 pb^{-1} of data [7]. The efficiency and resolution for high energy electromagnetic (EM) objects at D0 are superior to those for muons and so a search for LED in combined e^+e^- and $\gamma\gamma$ (di-EM) final states is superior to the dimuon channel. D0 and CDF have also published limits on M_D in the monophoton and monophoton plus monojet final states, respectively [8].

Events are collected using triggers requiring the presence of at least one EM calorimeter shower with the transverse momentum with respect to the beam axis, p_T , greater than 15 GeV. From these data we select e^+e^- and $\gamma\gamma$ events using criteria that do not distinguish photons from electrons. We require events with two EM showers with $p_T > 25 \text{ GeV}$. Showers are labelled CC (EC) if they are reconstructed in the central calorimeter (end cap calorimeters) with $|\eta| < 1.1$ ($1.5 < |\eta| < 2.4$), where pseudorapidity $\eta = -\ln[\tan(\theta/2)]$ and θ is the polar angle measured with respect to the proton beam direction. To reduce multijet background, we require at least one shower to be in the CC, so that selected events are either CC-CC (both showers in the CC) or CC-EC (one shower in the CC and the other in the EC). Each EM shower is required to be isolated, with less than 7% of the cluster energy in an annular cone $0.2 < \Delta\mathcal{R} < 0.4$ about the shower centroid, where $\Delta\mathcal{R} = \sqrt{(\Delta\eta)^2 + (\Delta\phi)^2}$ and ϕ is the azimuthal angle. We also demand the scalar sum of the p_T of all tracks

in the cone $0.05 < \Delta\mathcal{R} < 0.4$ be less than 2 GeV. Finally, we demand the EM shower profile be consistent with that of an electron or photon using a χ^2 test and that 97% of the shower energy be contained in the EM calorimeter.

The efficiencies for the electron and the photon selection criteria are determined from the same data set used for the event selection. We estimate separately the efficiencies for the χ^2 requirement on the EM shower shape, the isolation requirements based on $\Delta\mathcal{R}$, and for all calorimeter-based high- p_T triggers relevant to this analysis. In order to estimate the different efficiencies, we select a sample of di-EM events satisfying very loose EM identification requirements with invariant mass within $\pm 40 \text{ GeV}$ around Z boson mass. For each of these di-EM candidate events we estimate the efficiency as a function of η versus p_T using the tag and probe method [9]. This efficiency is then applied to Monte Carlo simulation samples.

The irreducible background to the LED signal is from SM e^+e^- and $\gamma\gamma$ production, while instrumental background arises from multijet and $\gamma + \text{jet}$ events with jets misidentified as EM objects. To model the invariant mass distribution of the physics backgrounds, we use the PYTHIA [10] event generator using the CTEQ6L1 parton distribution functions [11], followed by a GEANT-based [12] detector simulation and reconstruction with the same algorithms as applied to data. The next-to-leading order (NLO) effect for both e^+e^- and $\gamma\gamma$ is taken into account by multiplying the leading order (LO) cross section by a mass independent k -factor of 1.34 [13].

We generate the LED signal for $2 \leq n_d \leq 7$ and 33 different values of M_s using a parton level generator [14]. Following [4], we assume $Br(G_{KK} \rightarrow \gamma\gamma)/Br(G_{KK} \rightarrow e^+e^-) = 2$. In order to model the effects of detector resolution and initial state radiation (ISR), we generate LED+SM and SM-only events separately to obtain the parton level distributions of the di-EM invariant mass versus the cosine of the scattering angle in the centre of mass frame of the two EM candidates ($|\cos\theta^*|$) for each value of M_s and n_d considered. The ratio of the LED+SM and SM distributions are obtained for all values of M_s and n_d . Standard model events generated with the detailed GEANT-based Monte Carlo simulation are weighted by this ratio to model the effect of an LED signal. We reweight the shape of the SM to simulate the LED signal, keeping the overall normalization as in the pure SM case. By normalizing to the Z boson production cross section (NNLO), where the signal contribution is negligible, we reduce the fractional uncertainty on the product of the efficiency and integrated luminosity.

To estimate the normalization of the multijet background, we fit the di-EM invariant mass distribution of the selected data events with a linear combination of the physics and instrumental background distributions. The shape of the invariant mass distribution for the instrumental background is estimated from data events with EM energy clusters that fail the χ^2 requirement for the shower profile. This fit is performed in the mass range $60 - 140 \text{ GeV}$ where we expect no contribution from LED. We obtain separate fits for CC-CC and

TABLE I: Number of events observed and expected from SM processes in different mass windows for CC-CC and CC-EC events. The individual contributions to the total SM expectation from multijet, e^+e^- and $\gamma\gamma$ are also shown separately.

Mass (GeV)	CC-CC					CC-EC				
	Data N	Total Background $N_b \pm N_b^{sys}$	Multijet (MJ) $N_{MJ} \pm N_{MJ}^{sys}$	e^+e^- $N_{e^+e^-}$	$\gamma\gamma$ $N_{\gamma\gamma}$	Data N	Total Background $N_b \pm N_b^{sys}$	Multijet (MJ) $N_{MJ} \pm N_{MJ}^{sys}$	e^+e^- $N_{e^+e^-}$	$\gamma\gamma$ $N_{\gamma\gamma}$
240–290	61	67 ± 8	22 ± 3.1	30	15	144	171 ± 34	115 ± 34	34	21
290–340	30	28 ± 4	7 ± 1	14	7	52	55 ± 11	35 ± 11	12	8
340–400	21	15 ± 2	3 ± 1	7	5	21	23 ± 5	12 ± 4	7	4
400–500	9	9 ± 1	1.4 ± 0.3	5	3	12	9 ± 2	4 ± 2	3.3	1.2
500–600	1	3.6 ± 1.2	0.14 ± 0.09	2.4	1.1	2	1.5 ± 0.4	0.6 ± 0.2	0.73	0.18
600–1000	2	1.3 ± 0.1	0.11 ± 0.06	0.67	0.53	0	0.35 ± 0.07	0.03 ± 0.04	0.24	0.08

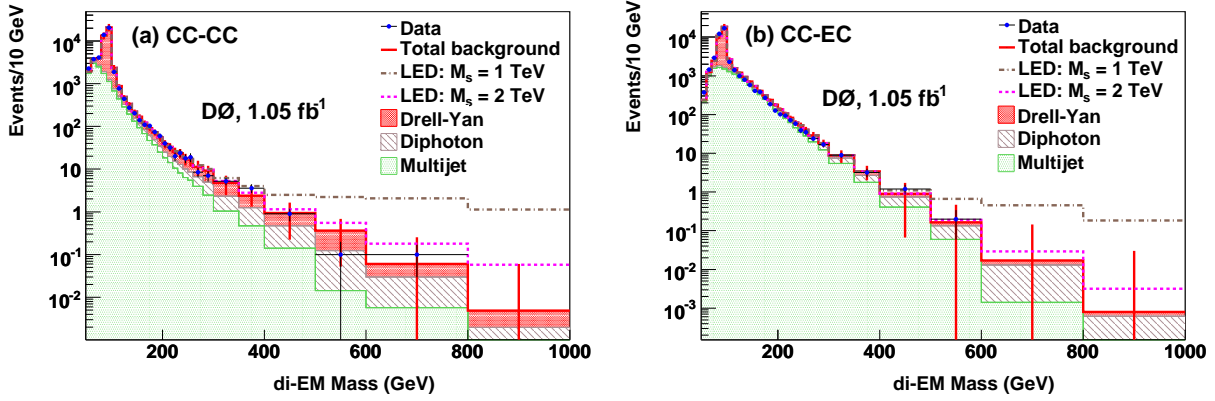


FIG. 1: The di-EM invariant mass distributions for CC-CC (a) and CC-EC (b) events. The data are shown by points with error bars, the filled histograms represent the Drell-Yan, diphoton and multijet backgrounds, and the solid line represents the total background. The broken lines show the invariant mass distributions for two different values of M_s for $n_d = 4$. The error bars for the total background include both statistical and systematic uncertainties.

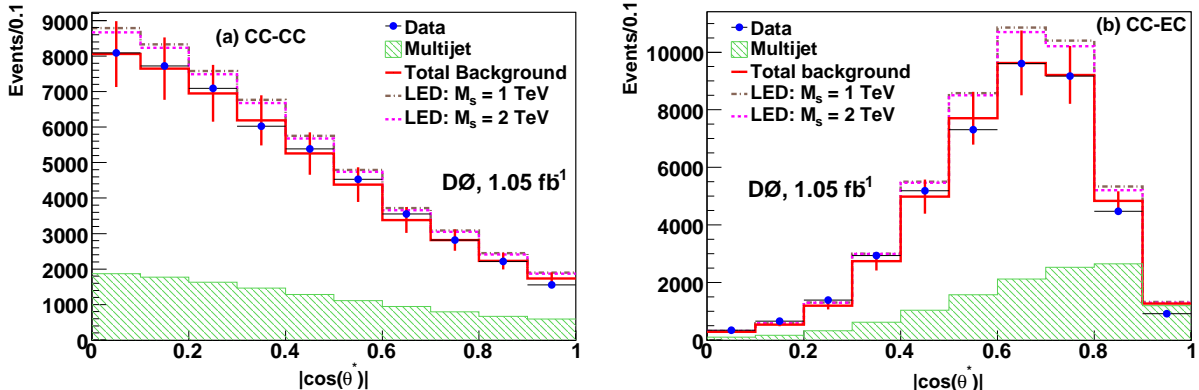


FIG. 2: The distributions of the center-of-mass scattering angle $\cos \theta^*$ of the two final state EM candidates in CC-CC (a) and CC-EC (b) events. The data are shown by points with error bars, the filled histogram represent the multijet background, and the solid line represents the total background. The broken lines show the $\cos \theta^*$ distributions for two different values of M_s for $n_d = 4$. The error bars for the total background include both statistical and systematic uncertainties.

CC-EC events. From the fits we determine the fraction f_{MJ} of the multijet contribution to the total background in the mass range $60 - 140$ GeV to be $f_{MJ} = 0.22 \pm 0.03$ in CC-CC events and $f_{MJ} = 0.24 \pm 0.07$ in CC-EC events. We extrapolate the total background using the fitted value of f_{MJ} to determine the expected number of background events with invariant mass above 140 GeV in both the CC-CC and CC-EC configurations. Table I shows the numbers of events in different mass ranges for CC-CC and CC-EC where we would

expect the LED signal to appear. The number of events is consistent with the number of expected events from the SM expectation. Figure 1(a) shows the invariant mass distribution for CC-CC events and Fig. 1(b) for CC-EC events. The distributions of $|\cos \theta^*|$ are shown in Fig. 2 for CC-CC and CC-EC both for data and the background model. We find that the total background distribution for the invariant mass and $|\cos \theta^*|$ is consistent with the data within statistical and systematic uncertainties.

Most of the systematic uncertainties on the background model are dependent on the invariant mass. The dominant uncertainty arises from the efficiency of the χ^2 cut on the shower profile used to estimate multijet background (13% of the background itself in CC-CC and 30% in CC-EC). The systematic on the LED modeling is dominated by uncertainties on the choice of parton distribution functions [(1–19)% in CC-CC and (1.5–12)% in CC-EC]. All the other signal uncertainties are correlated to SM background uncertainties due to the technique used to generate our LED signal. Table II summarizes the dominant background and signal uncertainties taken into account in calculating the limit on M_s . The NLO k-factor uncertainty refers to the uncertainty due to choice of PDF, renormalization and factorization scale.

TABLE II: Systematic uncertainties (in %) on the predicted numbers of signal and background events considered in calculating the limit on M_s .

	CC-CC	CC-EC
Signal only		
Acceptance	1–19	1.5–12
Luminosity		4
Signal and background		
Trigger + EM selection	6	5
Energy scale	5–13	0.3–3.5
Energy resolution	0.3–1.7	0.2–3.5
NLO k-factor		3–10
k-factor mass dependence		5
PDF		5.5–9
Background only		
Multijet	13	30

The two-dimensional distribution of the invariant mass and $|\cos \theta^*|$ for the observed dielectron and diphoton events is compared with the corresponding distributions expected from SM physics and instrumental background, and the LED signal for M_s ranging from 1 TeV to 3 TeV for a given n_d . The posterior probability density $P(M_s | \text{Data})$ given the number of observed events in the k^{th} mass bin and $l^{th} \cos \theta^*$ bin, $N_{\text{obs}}^{k,l}$, is then computed using a Gaussian prior for the SM plus multijet background. Evidence of large extra dimensions with a given M_s will appear as a peak in $P(M_s | \text{Data})$ distribution. In the absence of signal we proceed to estimate the lower limit on M_s using the semi-frequentist CLs method [15], which is based on computation of a log likelihood ratio. Both the expected and observed limits on M_s at the 95% C.L. are calculated. Systematic uncertainties in the signal and background distributions are taken into account in this calculation, with their correlations properly included. The distribution of the ratio of the observed (expected) upper limit at the 95% C.L. limit to the predicted cross section as a function of M_s is used to extract the observed (expected) limit on M_s for $n_d = 7$ to $n_d = 2$.

For the n_d independent GRW formalism, we calculate the observed(expected) limit on M_s of 1.62(1.66) TeV. We obtain the observed limits on M_s at the 95% C.L. in the HLZ formalism (sub-leading, n_d dependent) ranging from 1.29 to

TABLE III: Observed and expected lower limits at the 95% C.L. on the effective Planck scale, M_s , in TeV.

	GRW	HLZ					
		n_d	2	3	4	5	6
Obs.	1.62		2.09	1.94	1.62	1.46	1.36
Exp.	1.66		2.16	2.01	1.66	1.49	1.38
							1.29
							1.31

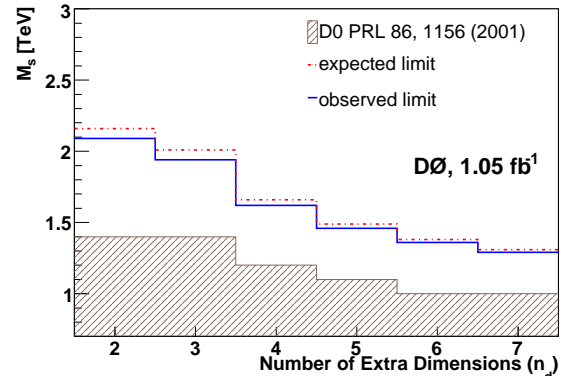


FIG. 3: Observed and expected limits on the effective Planck scale, M_s , in the di-EM channel along with previously published limits in di-EM channel.

2.09 TeV for $n_d = 7$ to $n_d = 2$. Both the observed and expected limits on M_s , for different formalisms and for six different n_d are summarized in Table III. The observed and expected limits on M_s for a given number of extra dimensions are found to be similar. The present limits are a significant improvement over the published limit [6]. Figure 3 summarizes the observed and expected limits on M_s along with the previously published limits on M_s in the di-EM channel.

In summary, we have performed a dedicated search for large extra spatial dimensions by looking for effects of virtual Kaluza-Klein graviton in the dielectron and diphoton channels using 1.05 fb^{-1} of data collected by D0 detector. We see no evidence of excess over the standard model prediction and set limits at 95% C.L. on the effective Planck scale at 2.09(1.29) TeV for 2(7) extra dimensions. These are presently the most restrictive limits on large extra dimensions.

We thank the staffs at Fermilab and collaborating institutions, and acknowledge support from the DOE and NSF (USA); CEA and CNRS/IN2P3 (France); FASI, Rosatom and RFBR (Russia); CNPq, FAPERJ, FAPESP and FUNDUNESP (Brazil); DAE and DST (India); Colciencias (Colombia); CONACYT (Mexico); KRF and KOSEF (Korea); CONICET and UBACyT (Argentina); FOM (The Netherlands); STFC (United Kingdom); MSMT and GACR (Czech Republic); CRC Program, CFI, NSERC and WestGrid Project (Canada); BMBF and DFG (Germany); SFI (Ireland); The Swedish Research Council (Sweden); CAS and CNSF (China); and the Alexander von Humboldt Foundation (Germany).

[a] Visitor from Augustana College, Sioux Falls, SD, USA.

[b] Visitor from The University of Liverpool, Liverpool, UK.

- [c] Visitor from Rutgers University, Piscataway, NJ, USA.
 - [d] Visitor from II. Physikalisches Institut, Georg-August University, Göttingen, Germany.
 - [e] Visitor from Centro de Investigacion en Computacion - IPN, Mexico City, Mexico.
 - [f] Visitor from ECFM, Universidad Autonoma de Sinaloa, Culiacán, Mexico.
 - [g] Visitor from Helsinki Institute of Physics, Helsinki, Finland.
 - [h] Visitor from Universität Bern, Bern, Switzerland.
 - [i] Visitor from Universität Zürich, Zürich, Switzerland.
 - [‡] Deceased.
- [1] N. Arkani-Hamed, S. Dimopoulos and G. Dvali, Phys. Lett. B **429**, 263 (1998); I. Antoniadis, N. Arkani-Hamed, S. Dimopoulos, and G. Dvali, Phys. Lett. B **436**, 257 (1998); N. Arkani-Hamed, S. Dimopoulos and G. Dvali, Phys. Rev. D **59**, 086004 (1999); N. Arkani-Hamed, S. Dimopoulos, and J. March-Russell, Phys. Rev. D **63**, 064020 (2001).
- [2] J. L. Hewett, Phys. Rev. Lett. **82**, 4765 (1999); K. Cheung, Phys. Lett. B **460**, 383 (1999); K. Cheung and G. Landsberg, Phys. Rev. D **62**, 076003 (2000); K. Cheung, Phys. Rev. D **61**, 015005 (2000); O. J. P. Eboli et al, Phys. Rev. D **61**, 094007 (2000).
- [3] G. Giudice, R. Rottazz and J. Wells, Nucl. Phys. **B544**, 3 (1999), and revised version arXiv:hep-ph/9811291.
- [4] T. Han, J. Lykken and R. Zhang, Phys. Rev. D **59**, 105006 (1999), and revised version arXiv:hep-ph/9811350.
- [5] V. M. Abazov *et al.* (D0 Collaboration), Nucl. Instrum. Methods in Phys. Res. A **565**, 463 (2006).
- [6] B. Abbott *et al.* (D0 Collaboration), Phys. Rev. Lett. **86**, 1156 (2001).
- [7] B. Abbott *et al.* (D0 Collaboration), Phys. Rev. Lett. **95**, 161602 (2005).
- [8] B. Abbott *et al.* (D0 Collaboration), Phys. Rev. Lett. **101**, 011601 (2008); T. Aaltonen *et al.* (CDF Collaboration), arXiv:0807.3132 [hep-ex], submitted to Phys. Rev. Lett.
- [9] B. Abbott *et al.* (D0 Collaboration), Phys. Rev. D **76**, 012003 (2007).
- [10] T. Sjöstrand, S. Mrenna and P. Skands, JHEP **0605**, 026 (2006); we used version 6.323.
- [11] J. Pumplin *et al.*, JHEP **0207**, 012 (2002); D. Stump *et al.*, JHEP **0310**, 046 (2003).
- [12] R. Brun and F. Carminati, CERN Program Library Long Writeup W5013, 1993 (unpublished).
- [13] P. Mathews, V. Ravindran, K. Sridhar and W. L. van Neerven, Nucl. Phys. **B713**, 333 (2005); R. Hamberg, W.L. van Neerven and T. Matsuura, Nucl. Phys. **B359**, 343 (1991) [Erratum-ibid. **B644**, 403 (2002)].
- [14] K. Cheung and G. Landsberg, Phys. Rev. D **62**, 076003 (2000).
- [15] T. Junk, Nucl. Instrum. Methods. A **434**, 435 (1999); A. Read, “Modified Frequentist Analysis of Search Results(The CLS Method)”, CERN 2000-005 (2000); W. Fisher, FERMILAB-TM-2386-E (2007);